PLANT SCIENCE TODAY
ISSN 2348-1900 (online)
Vol x(x): xx–xx
https://doi.org/10.14719/pst.6744

HORIZON
e-Publishing Group
HePG

RESEARCH ARTICLE

Mushroom-mediated silver nanoparticle synthesis: characterisation, antimicrobial and antioxidant activities

Adiba Sharif Abdalrahman[1*] & Sara Qatan Suliaman[2]

[1]Department of Maternity and Obstetric Nursing, Sulaimani Technical Institute, Sulaimani Polytechnic University, Sulaimani 460 23, Iraq

[2]Department of Biology, College of Science, Tikrit University, Tikrit 340 01, Iraq

*Email: adiba.sharif@spu.edu.iq

OPEN ACCESS

ARTICLE HISTORY
Received: 17 December 2024
Accepted: 03 February 2025
Available online
Version 1.0 : 17 February 2025

Check for updates

Additional information
Peer review: Publisher thanks Sectional Editor and the other anonymous reviewers for their contribution to the peer review of this work.

Reprints & permissions information is available at https://horizonepublishing.com/journals/index.php/PST/open_access_policy

Publisher's Note: Horizon e-Publishing Group remains neutral with regard to jurisdictional claims in published maps and institutional affiliations.

Indexing: Plant Science Today, published by Horizon e-Publishing Group, is covered by Scopus, Web of Science, BIOSIS Previews, Clarivate Analytics, NAAS, UGC Care, etc See https://horizonepublishing.com/journals/index.php/PST/indexing_abstracting

CITE THIS ARTICLE
Abdalrahman AS, Suliaman SQ. Mushroom-mediated silver nanoparticle synthesis: characterisation, antimicrobial and antioxidant activities. Plant Science Today (Early Access). https:/doi.org/10.14719/pst.6744

Abstract

The use of biological agents for the synthesis of green nanoparticles has garnered significant attention, emerging as a promising approach in nanotechnology and materials science. In this study, silver nanoparticles were synthesised using an aqueous extract from cultivated mushrooms, including *Chlorophyllum agaricoides* PP410314, *Coriolopsis trogii* PP921338.1, *Ganoderma* sp. PP921328.1 and *Lentinus tigrinus* PP921339.1, grown on potato dextrose agar (PDA). The formation of these nanoparticles was confirmed through UV-visible spectroscopy, with maximum absorbance observed at 424 and 426 nm. Nanoparticles were characterised to assess their stability, shape, size and crystallinity using various analytical techniques, such as Fourier transform infrared (FTIR) spectroscopy, atomic force microscopy (AFM), scanning electron microscopy (SEM) and X-ray diffraction (XRD). The XRD pattern revealed 2θ values corresponding to silver nanocrystals, with average crystallite sizes of 25.31, 27.05, 28.98 and 31.42 nm. The antimicrobial activity of the synthesised nanoparticles was tested against various microorganisms, including *Escherichia coli* ATCC25922, *Pseudomonas aeruginosa* ATCC9027, *Staphylococcus aureus* ATCC6538 and *Candida albicans* ATCC10231, demonstrating a strong inhibitory effect. Furthermore, antioxidant assays confirmed that these nanoparticles exhibited significant activity, which increased with concentration, in comparison to vitamin C. Overall, the green synthesis approach successfully produces silver nanoparticles with robust antioxidant and antibacterial properties, which can be attributed to the bioactive molecules present on their surface.

Keywords

antimicrobial; antioxidant; characterisation; mushroom; silver nanoparticles

Introduction

Mushrooms are a type of macrofungi found globally. They are fleshy, spore-producing fruiting bodies that typically grow above ground on soil or other nutrient source. With a wide range of species, mushrooms have been a staple in human diets for thousands of years, with their consumption increasing in recent times. Edible mushrooms are commonly used for both nutritional and medicinal purposes (1,2). A wide range of metabolites of commercial value can be produced from mushrooms, which are also inexpensive substrates. Their well-documented biological properties include antiviral, antibacterial, antitumor, anti-inflammatory, antioxidant and anticancer activities (3).

Nanoparticles (NPs) are integral to nanotechnology, exhibiting advanced

properties influenced by factors such as size and morphology. These unique characteristics enable their application across diverse fields, including biomedicine, energy science, optics and healthcare (4). Nanoparticle syntheses methods are categorised into chemical, physical and biological approaches, with biological synthesis being the most promising (5). Chemical and physical approaches are often expensive, energy-intensive and reliant on hazardous reagents. The limitations of traditional methods have driven growing interest in biogenic synthesis due to biocompatibility and environmental sustainability (6, 7). The production of metallic nanoparticles using microorganisms such as bacteria, fungi, algae and plants has gained considerable attention (8).

Macrofungi, particularly mushrooms, offer an innovative and efficient platform for large-scale nanoparticle synthesis. Over the past 15 years, eco-friendly metallic nanoparticles, including silver (Ag), gold (Au), selenium (Se), iron (Fe), zinc sulphide (ZnS) and palladium (Pd), have been synthesised from various mushroom species. These macrofungi belong to genera such as *Pleurotus*, *Agaricus*, *Schizophyllum*, *Ganoderma*, *Coriolus* and *Volvariella* (9). Among them, silver nanoparticles (AgNPs) stand out for their chemical biocompatibility and broad-spectrum antimicrobial properties. AgNPs interact with microbial cell walls and membranes, potentially penetrating cells. They disrupt cellular structures within the cell, generate reactive oxygen species (ROS) and interfere with signal transduction pathways (10). Additionally, AgNPs are less likely to promote drug-resistant microbial strains, making them highly effective antimicrobial agents for combating infections in humans (11).

This study highlights the growing interest in mushroom cultivation due to its potential for producing bioactive compounds. Submerged cultivation in bioreactors, performed under regulated conditions, is deemed more consistent and dependable than fruiting body cultivation. Beneficial compounds are present in the cultured broth, mycelium and fruiting bodies of mushrooms. Their concentrations may fluctuate based on factors such as mushroom strain, cultivation methods, developmental stage, freshness, storage conditions and extraction processes (12). Different mushroom species contain a variety of bioactive substances. For example, important phenolic substances such as gallic acid, naringin and trans-cinnamic acid are found in *Chlorophyllum agaricoides* (13). Laccases, which have a variety of industrial uses, are produced by *Coriolopsis trogii* (14). Phenolic compounds known for their strong antibacterial and antioxidant properties, are abundant in *Lentinus tigrinus* (15). Medicinal mushrooms, particularly those from the *Ganoderma* genus, such as *Ganoderma lucidum*, contain bioactive compounds including triterpenes, steroids, phenols, nucleotides, glycoproteins and polysaccharides (16).

This study investigated the extracellular synthesis of AgNPs from silver nitrate ($AgNO_3$) using various mushrooms successfully cultivated on PDA. These specific mushroom species have either not been previously used or have been rarely utilised for this purpose. Characterisation of the synthesised nanoparticles was conducted using UV-vis spectrophotometry, FTIR spectroscopy, AFM, SEM and (XRD). Additionally, the antimicrobial and antioxidant activities of the nanoparticles were evaluated against various bacterial and fungal strains.

Materials and Methods

Materials and reagents

Mushroom samples were collected from Sulaimani Province, Iraq. The bacterial strains, including *Escherichia coli* ATCC25922, *Staphylococcus aureus* ATCC6538 and *Pseudomonas aeruginosa* ATCC9027 as well as fungal strain *Candida albicans* ATCC10231, were obtained from the Biology Department of the College of Science at Sulaimani University.

The study utilised various reagents and materials, 1X Tris-Borate-EDTA (TBE) buffer (OnSite Buffer Pack, China), AddPrep genomic DNA extraction kit (ADDBIO, Korea), 2XPCR Mastermix (HSTM Kit, China), Taq DNA polymerase (2.5U/µ) (HSTM Kit, China), 100bp DNA Ladder (GeNet Bio, Korea), agarose (Carl ROTH, Germany), $AgNO_3$ (Merck, Germany), Potatoes dextrose agar (Himedia, India), potato dextrose broth (PDB, Himedia, India), Muller-Hinton agar (Mastgrp, UK), Muller-Hinton broth (Mastgrp, UK), 2,2-diphenylpicrylhydrazyl (DPPH) (Sigma-Aldrich, USA), ascorbic acid (Sigma-Aldrich, USA) were used.

The following instruments were employed in this study, including a Thermo Cycler (TECHNE, USA), gel electrophoresis instrument (Constort E863, Belgium), a gel document system (BIO-RAD, USA), a shaker incubator (Bibby Scientific, UK), UV-visible spectrometer (Cary 60; Agilent, USA), an atomic force microscope (NT-MDT, Ntegra, Russia), a scanning electron microscope (SEM; Quanta 450, Thermo Fisher Scientific, USA), an FTIR spectrometer (Spectrum Two N, PerkinElmer, USA), an X-ray diffractometer (PAN Analytical, Netherlands) and Whatman No.1 filter paper (Ltd. Maidstone, England).

Sample collection and molecular identification of mushrooms

Wild mushrooms were collected from various regions within the Sulaimani Province of Iraq. Samples were harvested from various locations and different substrates. The samples were cultured on PDA and the cultivated mushrooms were identified through the amplification of the internal transcribed spacer (ITS) region of their ribosomal DNA (rDNA) using a primer set consisting of ITS1 (5´TCCGTAGGTGAACCTGCGG-3´) and ITS4 (5´TCCTCCGCTTATTGATATGC-3´) (17).

PCR reaction was performed for 35 cycles using a thermocycler (18). The Sanger method was employed for DNA sequencing with a 3500xl genetic analyser (Applied Biosystems). Nucleotide sequences were analysed utilising the Basic Local Alignment Search Tool (BLAST) and the database provided by the National Centre for Biotechnology Information (NCBI), http://www.ncbi.nlm.nih.gov/BLAST.

Mushroom cultivation and biomass preparation

Pure cultures of the isolated mushrooms were obtained using tissue culture techniques. Tissue samples were taken from the junction of the pileus and stem, ensuring they were uncontaminated. Subsequently, these samples were then

transferred to PDA and incubated at 25°C ± 2°C for 7 days. Following incubation, the tissue produced mycelium, which spread across the surface of the PDA (19).

For biomass preparation, a 0.5 cm disc of actively growing mycelium was transferred into a flask containing 100 mL of PDB and incubated at 27°C ± 2°C for 10 days in a shaker incubator set at 150 rpm (20). The fungal biomass was then collected using Whatman filter paper No. 1 and thoroughly washed with double distilled water 2–3 times to eliminate any remaining medium. A 20 g portion of the wet biomass was placed in a flask containing 100 mL of double-distilled water and incubated at 27°C for 5 days (21).

Synthesis of AgNPs from mushroom filtrate

A 5mM aqueous solution of $AgNO_3$ was prepared to synthesise AgNPs. Then, 90 mL of the 5 mM $AgNO_3$ solution was mixed with 10 mL of mushroom extract. The mixture was then incubated for 96 hours at room temperature. The formation of AgNPs was indicated by a color change to brown. A control flask containing only the $AgNO_3$ solution, without mushroom extract, was incubated under identical conditions (22).

Characterisation of AgNPs

The synthesis of AgNPs and the reduction of silver ions were verified using UV-visible spectroscopy. The samples were analysed by measuring the peak absorbance wavelength within the range of 250 to 800 nm (23). FTIR spectroscopy was used to identify biomolecules and functional groups present in the sample. The measurements were conducted at a spectral resolution of 4 cm^{-1} within the range of 450 to 4000 cm^{-1} (24).

AFM was used to investigate the surface topography of the AgNPs. The analysis involved scattering the material onto a small glass slide, which was then examined under the microscope (25). XRD analysis was conducted to study the formation, crystalline properties and quality of the AgNP powder. The X-ray diffractometer (PAN analytical X'Pert Pro) scanned at a rate of 1°/min across a 2θ range of 20° to 70°, utilising Cu-Kα radiation (λ = 1.54 Å). All samples were analysed with Highscore software and the diffraction patterns were collected within the 2θ range of 20° to 70°. The XRD analysis was conducted using an X'Pert Pro (PANalytical, Netherlands), equipped with a high-intensity Cu-Kα radiation source (λ = 0.154 nm, 40 mA, 40 kV) (26).

SEM was used to assess the two-dimensional structure and surface morphology of the AgNPs at high magnification. SEM functions by directing a beam of electrons onto a sample, resulting in the emission of secondary or backscattered electrons, which are then detected. The morphology and particle distribution were examined with a Quanta 450 (27).

Antimicrobial activity of AgNPs

The antimicrobial activity of four different AgNPs synthesised from *C. agaricoides* (CaAgNPs), *C. trogii* (CtAgNps), *Ganoderma sp.* (GsAgNPs) and *L. tigrinus* (LtAgNPs). The mushroom extracts and silver nitrate were evaluated against ATCC microorganisms (*E. coli* ATCC25922, *P. aeruginosa* ATCC9027, *S. aureus* ATCC6538 and *C. albicans* ATCC10231).

The bacterial and the fungal strains were inoculated into Mueller-Hinton broth (MHB) and incubated overnight at 37°C. The cultures were then diluted with fresh MHB media to attain an optical density of 0.1 at 600 nm, equivalent to 10^8 cells/ mL. For each microorganism, 100 µL of the culture was combined with 100 µL of AgNPs, mushroom extract, or silver nitrate at varying concentrations. Following, a 15 min incubation at 37°C, the mixture was transferred onto Mueller-Hinton agar plates. The plates were then subsequently incubated overnight at 37°C and microbial growth was monitored to assess inhibition (28, 29).

DPPH (1, 1-diphenyl-2-picrylhydrazyl) antioxidant assays

The antioxidant efficacy of CaAgNPs, CtAgNPs, GsAgNPs and LtAgNPs was evaluated utilising the DPPH (1,1-diphenyl-2-picrylhydrazyl) free radical scavenging assay. One milliliter of each AgNPs, prepared in 10 % DMSO at varying concentrations (12.5 µg/mL, 25 µg/mL, 50 µg/mL, 100 µg/mL and 200 µg/mL), was combined with a standard solution of DPPH and DMSO. Subsequently, 1 mL of 0.3 mM DPPH solution was added to the mixture under dark conditions and incubated for 30 min. The absorbance was quantified at 517 nm using a UV-Vis spectrophotometer (UV-1800 Shimadzu).

Ascorbic acid was used as a reference standard at the same concentrations (12.5 µg/mL, 25 µg/mL, 50 µg/mL, 100 µg/mL and 200 µg/mL) (30). The inhibition % was determined using the subsequent formula:

$$\% \text{ inhibition} = \frac{Abs_{(Control)} - Abs_{(sample)} \times 100}{Abs_{(Control)}} \quad \text{(Eqn. 1)}$$

Statistical analysis

The data were analysed using the Minitab software and an ANOVA test was performed. Tukey's post hoc test and Duncan's multiple range test were applied to assess significant differences between group variances. A significance threshold of $p < 0.05$ was used to determine statistical significance.

Results and Discussion

The molecular identification of the four isolated mushroom species was conducted by sequencing their nucleotide and analysing them using the BLAST search tool (NCBI) against the comprehensive GenBank nucleotide database. The BLAST results indicated that *L. tigrinus* accession number (PP921339.1) was identified with 100 % certainty, *Ganoderma sp.* (PP921328.1) with 99 % certainty, *C. trogii* (PP921338.1) with 100 % certainty and *C. agaricoides* (PP410314). Molecular identification and DNA barcoding serve as powerful tools in fungal taxonomy, facilitating the precise identification of mushroom species. However, accurate identification also necessitates a thorough examination of their phenotypic traits, including macroscopic attributes of the fruiting body and microscopic details of the spores (31).

In this study, the selected mushrooms were used to

synthesise unique AgNPs, which, to the best of our knowledge, have not previously been recorded for this purpose. A visible colour changes from light yellow to dark brown was observed, indicating the formation of AgNPs. The yellowish-brown colour arises due to the excitation of surface plasmon vibrations, a phenomenon referred to as surface plasmon resonance (SPR) (32). In contrast, the control silver nitrate solution, which lacked mushroom extract, exhibited no colour change (Fig. 1A). UV-visible spectroscopy is widely used for characterising nanoparticle formation and properties. In nanoparticles, electron oscillations are confined to specific vibrations, which are influenced by the particle's size and shape (33).

The UV absorption spectra of the AgNP solution revealed a peak in the visible range at 424 nm for CaAgNPs and CtAgNPs while GsAgNPs and LtAgNPs exhibited a peak at 426 nm, as shown in (Fig. 1B). These findings align with previous reports indicating that the characteristic peak for AgNP formation occurs within the range of 422-426 nm, with estimated nanoparticle sizes between 2 and 40 nm (34).

FTIR analysis was performed on the synthesised AgNPs to determine the key functional groups or biomolecules on their surface that may contribute to their synthesis and stabilisation (35). The FTIR spectrum (Fig. 2) displayed multiple peaks. The broad peak at 3437 cm^{-1} is indicative of either N-H stretching from amines (found in proteins or enzymes) or O-H stretching from hydroxyl groups (found in alcohols or water). These functional groups, likely derived from biomolecules in the mushroom extracts, are believed to stabilise the NPs. Similar findings have been reported in previous studies (36). A peak between 2071 and 2081 cm^{-1} may suggest the presence of specific biomolecules involved in the reduction and capping of the NPs. The observed peaks in biosynthesised AgNPs have been attributed to O-H stretching at 3428 cm^{-1}, C-O at 2071 cm^{-1}, N-H bending at 1634 cm^{-1}, C-N at 1067 cm^{-1} and C-Br at 687 cm^{-1}, as noted in earlier research (37). Similar results have been documented for three mushroom species, all of which exhibited a peak at 2079 cm^{-1}, indicating a shared metabolic component associated with these fungi (38).

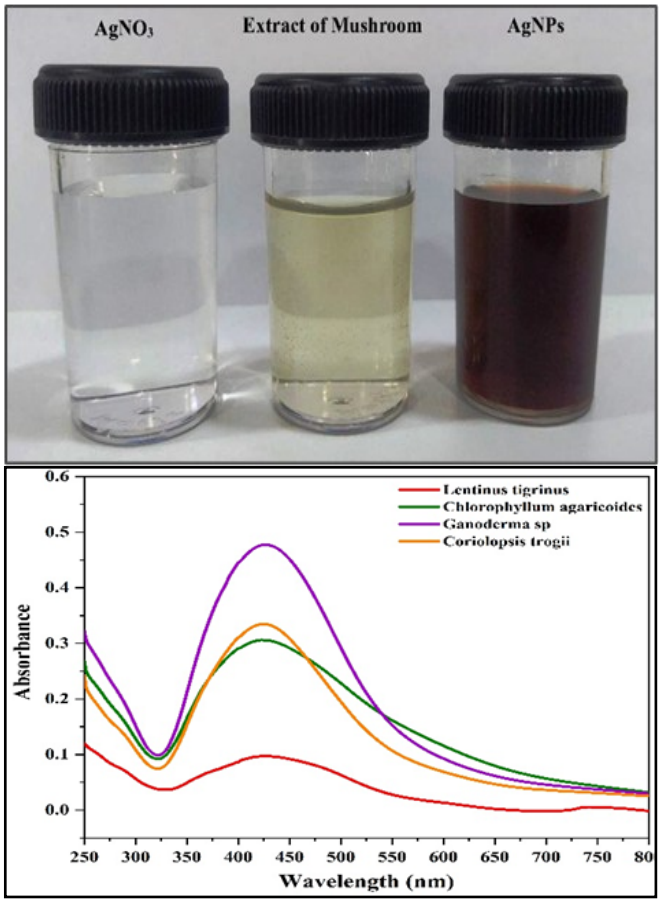

Fig. 1. **A**-Biosynthesis of AgNPs reaction of colour change after exposure to $AgNO_3$, **B**- UV-Visible spectroscopy of AgNPs synthesised from different mushroom extract.

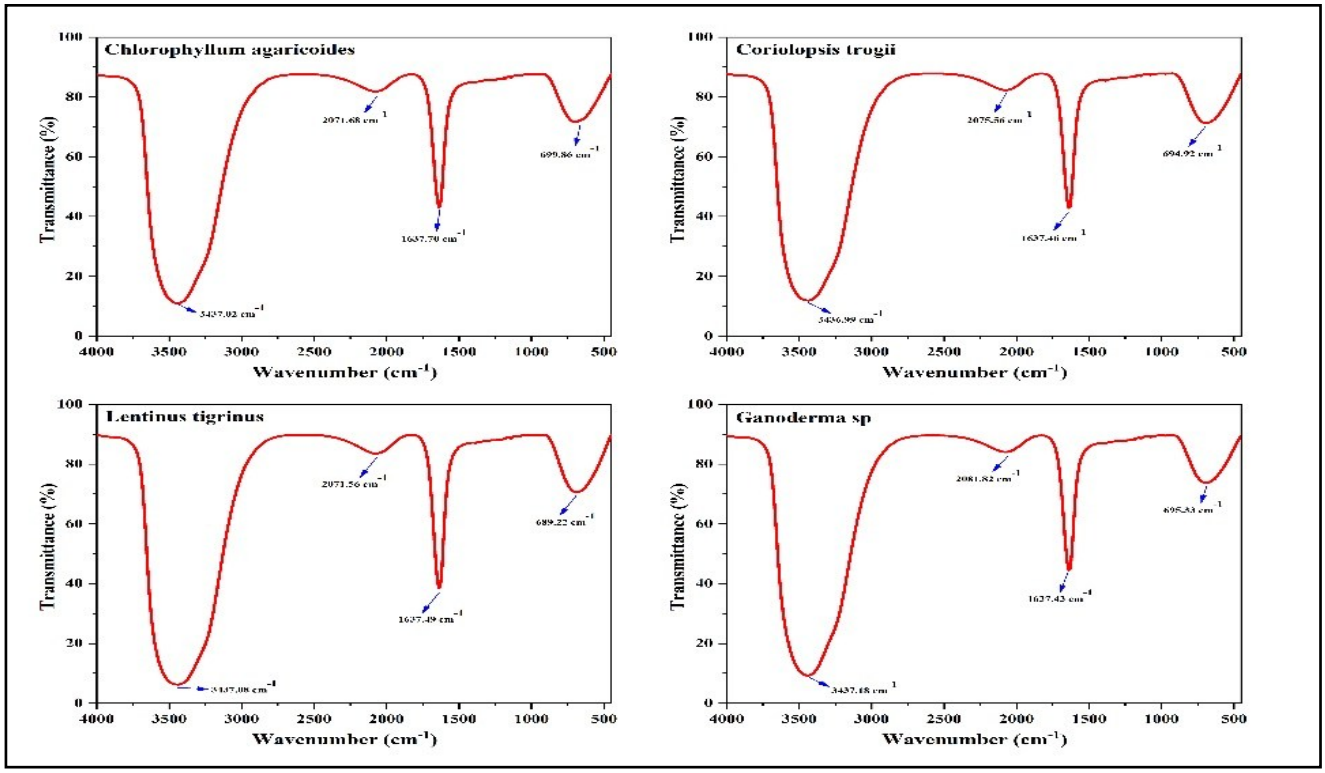

Fig. 2. FTIR of AgNPs synthesized using different mushroom extract.

A peak observed at 1637 cm^{-1} is associated with either C=C stretching in aromatic compounds or C=O stretching vibrations of amide groups typically found in proteins, suggesting that these proteins act as capping agents for the AgNPs. The FTIR spectra of green synthesised AgNPs contain many absorption peaks, with three significant peaks identified at 3310, 1637 and 671 cm^{-1}. The absorption band observed at 1637 cm^{-1} is due to carbonyl (C=O) groups, as previously reported (39). Peaks between 689 and 699 cm^{-1} may correspond to out-of-plane C-H deformations or C-H bending vibrations in aromatic rings, which suggest the presence of secondary metabolic compounds in the mushroom extracts, as demonstrated in previous studies (40).

An AFM image of the four synthesised AgNPs is shown in Fig. 3. The AFM results show a wide range of nanoparticle sizes and surface features, each appropriate for a particular use. The AgNPs exhibit varying degrees of roughness, ranging from extremely smooth to low and moderate roughness, which suggesting a well-organised and consistent nanoparticle structure. A study reported that similar AFM results for AgNPs synthesized from *Agaricus bisporus* mushroom (41). AFM facilitates the analysis of nanomaterial dimensions and morphologies under physiological conditions and enables observing dynamic interactions among nanomaterials inside biological settings (42).

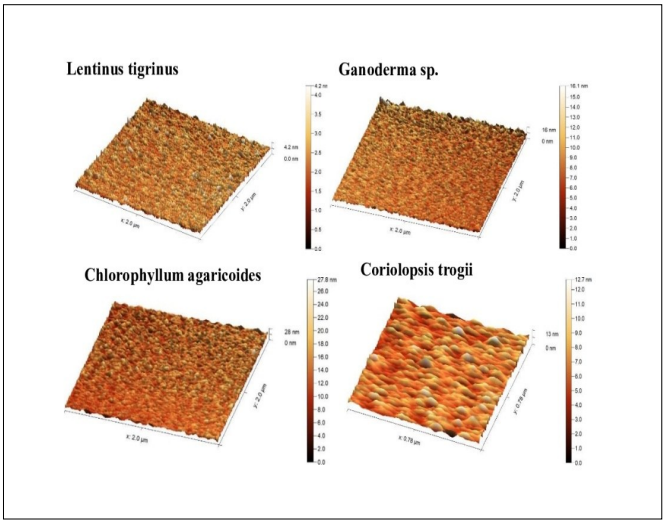

Fig. 3. Atomic force microscopy of silver nanoparticles synthesised from different mushroom extract.

The X-ray diffraction peak patterns of CaAgNPs, CtAgNPs, GsAgNPs and LtAgNPs are illustrated in (Fig. 4). The peak patterns confirm the formation of AgNPs exhibiting a face-centred cubic (fcc) crystal structure, characterised by the (F m -3 m) space group, which is consistent with ICSD 98-018-0879.

The crystallite sizes of the synthesised AgNPs were determined using the Debye-Scherrer equation, as shown below (43):

$$D = \frac{k\,\lambda}{\beta \cos\theta} \qquad \text{(Eqn. 2)}$$

where D is the crystallite size, k is the geometric factor, β is the full width at half maximum (FWHM) and θ is the Bragg angle.

Additional structural parameters, including dislocation density, lattice strain, X-ray density and specific surface area, were calculated using the following relations (44):

$$\delta = \frac{1}{D^2} \qquad \text{(Eqn. 3)}$$

$$\varepsilon = \frac{4}{\beta \tan\theta} \qquad \text{(Eqn. 4)}$$

$$\rho_x = \frac{n\,M_w}{N_A\,V} \qquad \text{(Eqn. 5)}$$

$$SSA = \frac{6000}{D\,\rho_x} \qquad \text{(Eqn. 6)}$$

where d is the dislocation, e is the lattice strain, n is the number of atoms occupying a unit cell (for the fcc structure, n=4), M_w is the molecular weight of a silver atom, N_A is Avogadro's number (N_A=6.023×10^{23} mol^{-1}), ρ_x is the X-ray density and SSA is the specific surface area. All calculated values are presented in Table 1.

The XRD patterns exhibit three characteristic peaks at (111), (200) and (220), confirming the crystalline nature of AgNPs (Fig. 4). These peaks are present in all samples except for GsAgNPs, which display only two peaks. Similar XRD patterns have been reported for AgNPs synthesized using *L. squarrosulus*, *G. lucidum* and *Pleurotus tuberregium*, where three characteristic peaks corresponding to the (111), (200) and (220) crystallographic planes were observed (39). The (111) peaks, identified in all four samples, is associated with enhanced antibacterial activity. The close-packed atomic layers on the lower surfaces of anisotropically shaped AgNPs contribute to an extensive reactive surface area, significantly boosting their antibacterial effectiveness (45). Other peaks observed in the XRD pattern indicate impurities

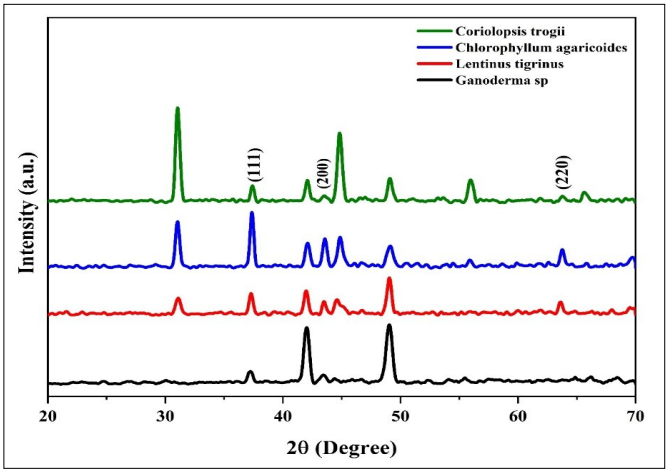

Fig. 4. X-ray diffraction (XRD) pattern of AgNPs synthesised by mushrooms.

Table 1. Crystallite size (D), dislocation (δ), strain (ε), lattice parameter (a), X-ray density (ρx) and surface area (SSA) of silver nanoparticle

Samples	D (nm)	δ (nm^{-2})	ε	a (nm)	(ρx) g/cm^3	SSA
CaAgNPs	28.98	0.001191	0.003732	0.4163	9.932	20.85
LtAgNPs	27.05	0.001366	0.004006	0.4171	9.875	22.46
GsAgNPs	31.42	0.001013	0.003455	0.4178	9.824	19.44
CtAgNPs	25.31	0.001561	0.004268	0.4158	9.964	23.79

within the samples. These peaks suggest the presence of residual mushroom metabolites on the surface of the NPs, which act as capping agents (46). Moreover, the crystallite sizes of CtAgNPs, LtAgNPs, CaAgNPs and GsAgNPs were calculated to be 25.31, 27.05, 28.98 and 31.42, respectively.

SEM was employed to quantify the dimensions of diverse AgNPs at the micro- (10^{-6}) and nano- (10^{-9}) scales, as well as to analyse their topography and morphology. When the sample surface is exposed to a high-energy electron beam from the SEM, the emitted backscattered electrons elucidate the distinctive properties of the material (47). The SEM images of the four synthesised AgNPs revealed spherical particles with varying diameters, along with some larger particles resulting from aggregation. The observed aggregation is likely due to solvent evaporation during sample preparation (Fig. 5). Furthermore, impurities are present in all four samples, likely resulting from secondary metabolites from the mushroom extracts, as confirmed by XRD analysis. As the quantity of extract increased, the particle size increased with decreasing number of silver ions. This trend has been observed in SEM analysis of AgNPs synthesised from *Hebeloma excedens*, where the resulting AgNPs exhibited a spherical structure with a nearly homogeneous distribution (48)

The antimicrobial activity of AgNPs biosynthesised from various mushroom species against a range of microorganisms is shown in (Fig. 6A and 6B). The four samples exhibited strong antimicrobial effects on the selected microorganisms, with activity ranging from a means of 6 % to 34 %. According to statical analysis, *E. coli* ATCC25922 exhibited the highest susceptibility (Fig. 6B), with no growth at a mean of 6 % for CaAgNPs. Similarly, *P. aeruginosa* ATCC9027 showed complete inhibition at 6 % LtAgNPs, whereas GsAgNPs displayed inhibitory effects at a means of 16 %. No significant differences were observed among the Gram-negative bacteria, except in the case of GsAgNPs, where a significant difference was noted (Fig. 6A). In contrast, inhibition of the Gram-positive *S. aureus* ATCC6538 was observed at a lower percentage, with a means of 18% for LtAgNPs. These findings suggest that Gram-negative bacteria are generally more susceptible to AgNPs than gram-positive bacteria, with a highly significant difference between the two groups, consistent with previous reports (23, 49).

Similar findings were reported where green-synthesised silver nanoparticles (AgNPs) displayed notable antibacterial activity against both Gram-positive and Gram-negative bacteria (50). The study showed that Gram-negative bacteria were more sensitive to AgNPs, exhibiting a dose-dependent response. At a concentration of 400 µg/ disk, *E. coli* demonstrated an inhibition zone of 17.3 ± 0.14 mm, while *Staphylococcus epidermidis* displayed a zone of 13.5 ± 0.49 mm. The substantial peptidoglycan layer in Gram -positive bacteria functions as a barrier, obstructing the entry of the AgNPs into the cell (51). However, another study found no conclusive evidence indicating a stronger antibacterial effect on Gram-negative bacteria than Gram-positive bacteria (52).

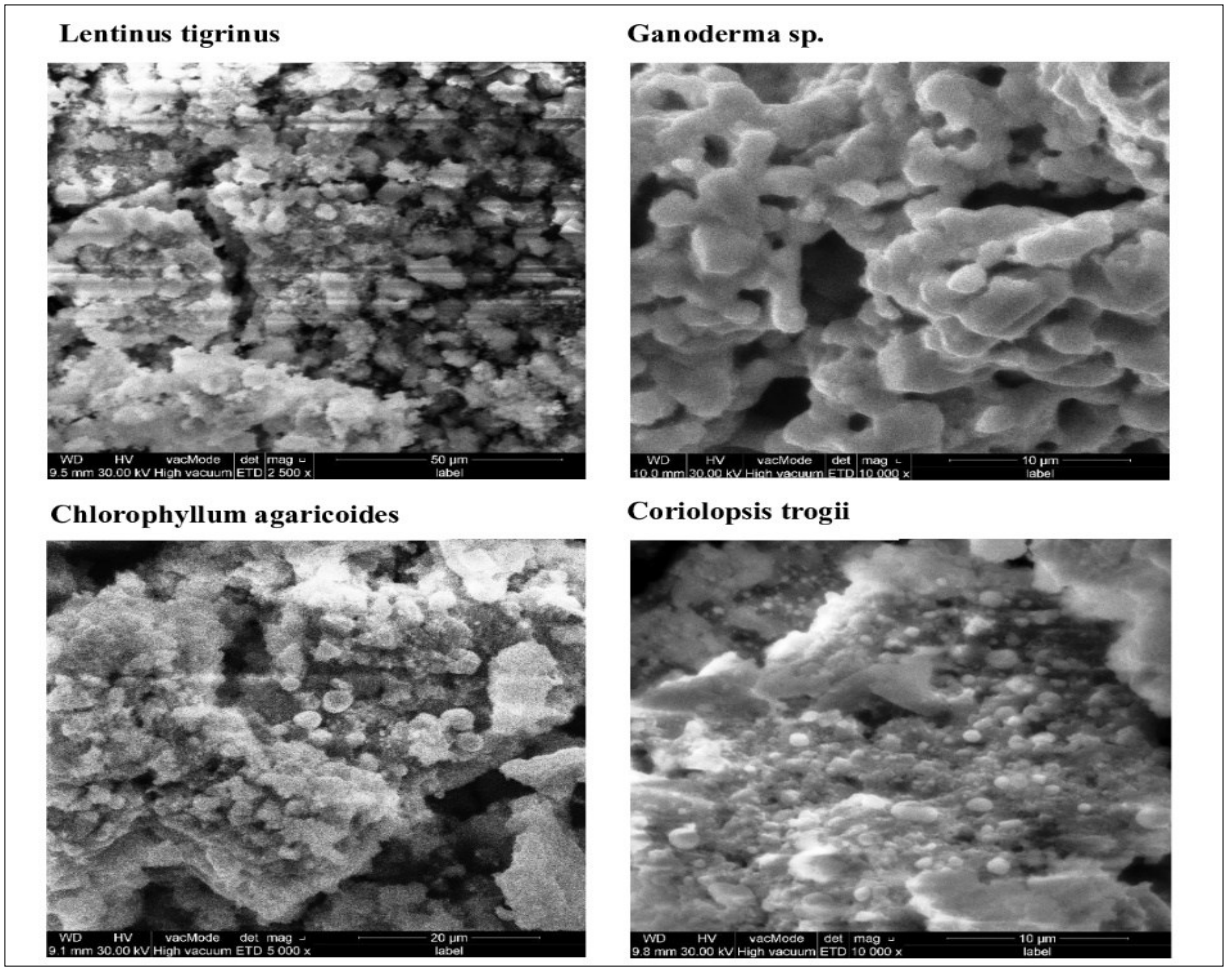

Fig. 5. Scanning electron microscopy (SEM) of synthesised AgNPs from different mushroom.

Regarding fungal inhibition, *C. albicans* ATCC10231 was greatly affected by different AgNPs, with statically significant differences observed among them. A study indicated that the inhibition of microorganisms increases with higher AgNP concentrations, significantly affecting *S. aureus*, *E. coli*, *K. pneumoniae* and *P. aeruginosa* (53). Several key physicochemical parameters, including nanoparticle size, shape, surface charge, concentration and colloidal stability influence the antimicrobial efficacy of AgNPs. Additionally, the antimicrobial capabilities of AgNPs are due to various mechanisms, including their ability to adhere to and penetrate microbial cells, generate ROS and free radicals and modulate microbial signal transduction pathways (54). The mushroom extracts alone exhibit no antimicrobial effect; in contrast, $AgNO_3$ demonstrated both antibacterial and antifungal activity against the selected microorganisms, with a low significant difference among them, consistent with findings reported (55).

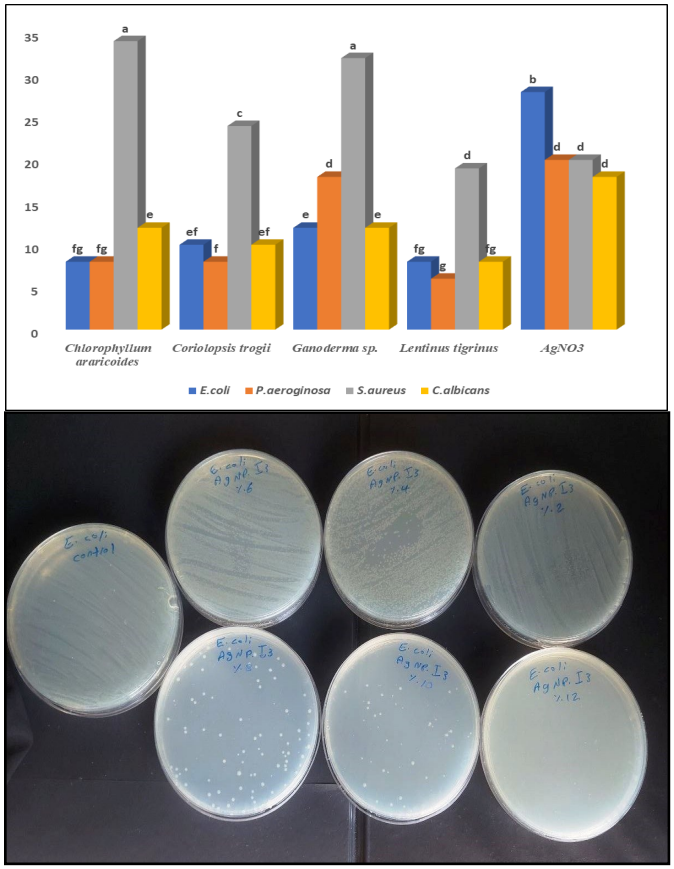

Fig. 6. A. Antimicrobial activity of AgNPs synthesised by mushrooms, (Note. Similar letters mean none significant difference, while different letters mean significant difference between them). **B.** Inhibiting growth of microorganisms by increasing % of AgNP.

The antioxidant activity of AgNPs was evaluated using the DPPH free radical assay. DPPH is a stable compound capable of being reduced by hydrogen or electron acceptance. DPPH free radical assays are widely used to evaluate antioxidant activity (56). The four distinct AgNPs exhibited significant free radical scavenging capabilities, as illustrated in (Fig. 7). Antioxidant activity increased AgNPs with rising concentrations, in alignment with previous studies (57, 58). The CaAgNPs exhibited scavenging activity like that of ascorbic acid with no significant difference between them, reaching a maximum activity of 75 % at a concentration of 200 µg/mL in the DPPH assay. CtAgNPs exhibited antioxidant activity reaching approximately 63 %, but a highly significant difference was observed when compared to ascorbic acid. The reducing power of a compound serves as a valuable indicator of its potential antioxidant activity, as it is linked to its ability to transfer electrons.

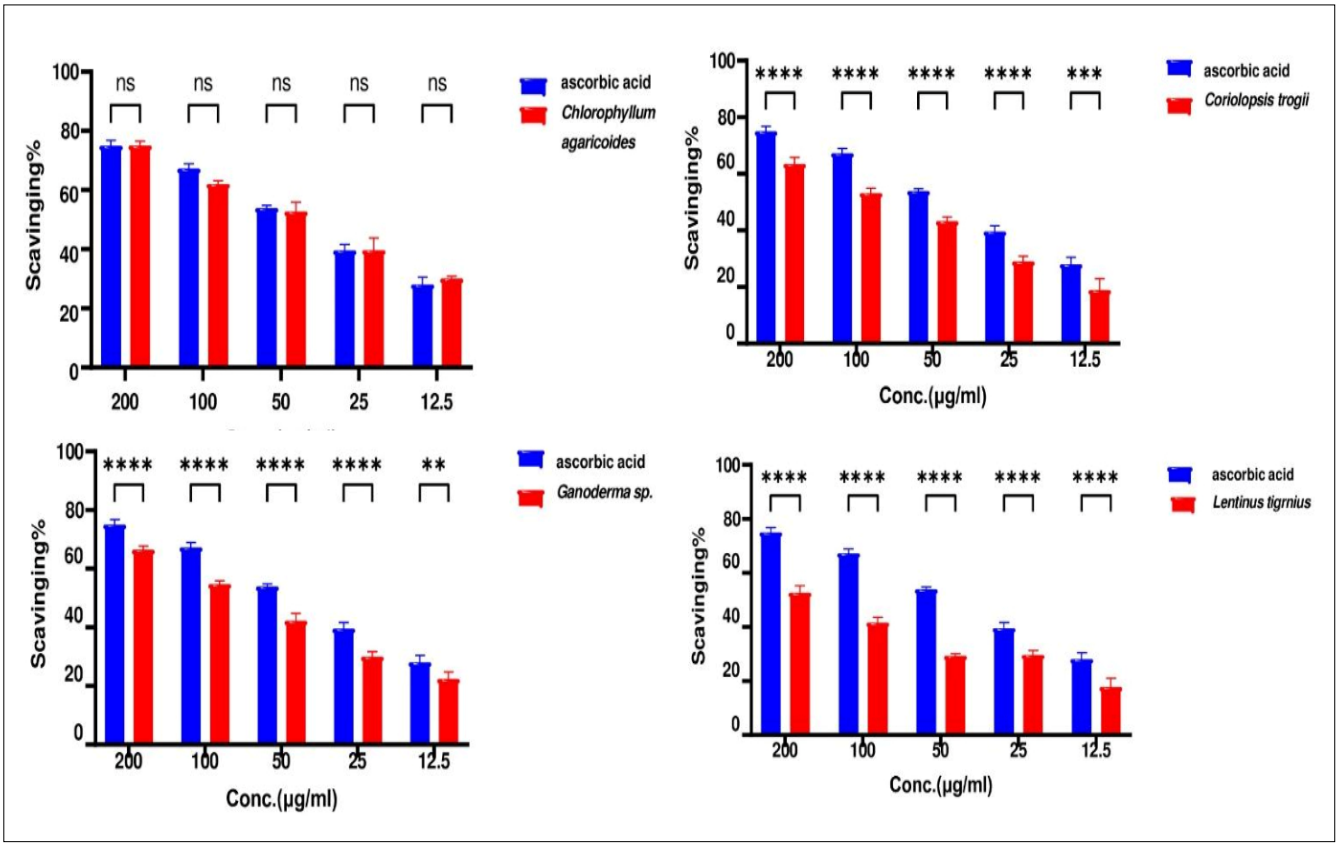

Fig. 7. Antioxidant activity of AgNPs synthesised by mushrooms (Note. ns= none significant difference. *indicate significant differences).

Conclusion

The eco-friendly synthesis of AgNPs has attracted considerable interest among researchers due to its environmental benefits, improved safety, and economic efficiency relative to conventional chemical approaches. Consequently, AgNPs were synthesised utilising *C. agaricoides*, *C. trogii, Ganoderma sp*., and *L. tigrinus* cultivated on PDA media. The biosynthesised AgNPs displayed strong antimicrobial capabilities, highlighting their potential effectiveness against various pathogens. Additionally, they demonstrated considerable antioxidant activity, as evidenced by DPPH radical scavenging experiments. Notably, *C. agaricoides* and *C. trogii* have the strongest antioxidant activity.

This study's results suggest that AgNPs possess significant potential for application in medical devices and as antibacterial agents against multidrug-resistant bacteria. Furthermore, the two mentioned species serve as valuable natural sources of antioxidant compounds, providing a viable alternative to synthetic antioxidants for applications in industries like cosmetics, medicine and food production.

Acknowledgements

Authors wish to thank their sincere gratitude to the University of Tikrit and the Biology lab at Sulaimani University/ College of Medicine for providing all the necessary resources to conduct this work.

Authors' contributions

ASA and SQS has conducted the molecular identifications, synthesis of nanoparticles, characterizations study, antimicrobial, antioxidant activity, participated in data analysis, writing, editing and finalising the draft of manuscript. Authors read and approved the final manuscript.

Compliance with ethical standards

Conflict of interest: The authors state that there are no conflicts of interest concerning the publication of this article.

Ethical issues: None

References

1. Indumathi M, Ishwarya J. *In vitro* evaluation of antimicrobial activity of silver nanoparticle from edible mushroom. Int J Adv Res Biol Sci. 2022;9(5):164–70. http://dx.doi.org/10.22192/ijarbs.2022.09.05.018
2. Mirunalini S, Arulmozhi V, Deepalakshmi K, Krishnaveni M. Intracellular biosynthesis and antibacterial activity of silver nanoparticles using edible mushrooms. Not Sci Biol. 2012;(4):55–61. www.notulaebiologicae.ro
3. Alghuthaymi MA, Almoammar H, Rai M, Said-Galiev E, Abd-Elsalam KA. Myconanoparticles: synthesis and their role in phytopathogens management. Biotechnol Biotechnol Equip. 2015;29(2): 221–36. http://doi.org/10.1080/13102818.2015.1008194
4. Priyadarshni KC, Mahalingam PU. Antimicrobial and anticancer activity of silver nanoparticles from edible mushroom: a review. Asian J Pharm Clin Res, Innovare Academics Sciences. 2017;10(3) 37–40. http://doi.org/10.22159/ajpcr.2017.v10i3.16027
5. Gezaf SA, Hamedo HA, Ibrahim AA, Mossa MI. Mycosynthesis of silver nanoparticles by endophytic Fungi: Mechanism, characterization techniques and their applications. Microb Biosyst J. 2023; 7(2): 48–65. http://doi.org/10.21608/mb.2023.185718.1066
6. Vijayakumar G, Kim HJ, Jo JW, Rangarajulu SK. Macrofungal mediated biosynthesis of silver nanoparticles and evaluation of its antibacterial and wound-healing efficacy. Int J Mol Sci. 2024; 25(2):861. https://doi.org/10.3390/ijms25020861
7. Nirmala S, Siva R. Green synthesis of silver nanoparticles from *macrocybe gigantea* and its effect against food borne pathogens. Indian Journal of Science and Technology. Indian J Sci Technol. 2023;16(9):605–13. https://doi.org/10.17485/IJST/v16i9.2288
8. Vanaja M, Annadurai G. *Coleus aromaticus* leaf extract mediated synthesis of silver nanoparticles and its bactericidal activity. Applied Nanoscience (Switzerland). 2013;3:217–23. https://doi.org/10.1007/s13204-012-0121-9
9. Owaid MN, Naeem GA, Muslim RF, Oleiwi RS. Synthesis, characterization and antitumor efficacy of silver nanoparticle from *Agaricus bisporus* Pileus, Basidiomycota. Walailak J Sci & Tech 2020;17(2):75–87. https://doi.org/10.48048/wjst.2020.5840
10. Guilger-Casagrande M, Lima R de. Synthesis of silver nanoparticles mediated by fungi: a review. Front Bioeng Biotechnol. 2019;7:287. https://doi.org/10.3389/fbioe.2019.00287
11. Gudikandula K, Maringanti SC. Synthesis of silver nanoparticles by chemical and biological methods and their antimicrobial properties. J Exp Nanosci. 2016,11(9):714-21. http://doi.org/10.1016/j.onano.2017.07.002
12. Fogarasi M, Nemeș SA, Fărcaș A, Socaciu C, Semeniuc CA, Socaciu MI, et al. Bioactive secondary metabolites in mushrooms: A focus on polyphenols, their health benefits and applications. Food Bioscience. Elsevier Ltd; 2024; 62,105166. https://doi.org/10.1016/j.fbio.2024.105166
13. Kumlay AM, Koçak MZ, Koyuncu M, Güller U. Bioanalysis of total phenolic contents, volatile compounds and radical scavenging activities of three wild edible mushrooms. STUDIA UBB CHEMIA, LXVI. 2021;66(4):133–48. https://doi.org/10.24193/subbchem.2021.4.10
14. Mellere L, Bellasio M, Berini F, Marinelli F, Armengaud J, Beltrametti F. *Coriolopsis trogii* MUT3379: A novel cell factory for high-yield laccase production. Fermentation. 2024;10(7):376. https://doi.org/10.3390/fermentation10070376.
15. Dulay RMR, Miranda LA, Malasaga JS, Kalaw SP, Reyes RG, Hou CT. Antioxidant and antibacterial activities of acetonitrile and hexane extracts of *Lentinus tigrinus* and *Pleurotus djamour*. Biocatal Agric Biotechnol. 2017;9:141–44. https://doi.org/10.1016/j.bcab.2016.12.003
16. Martínez-Montemayor MM, Ling T, Suárez-Arroyo IJ, Ortiz-Soto G, Santiago-Negrón CL, Lacourt-Ventura MY, et al. Identification of biologically active *Ganoderma lucidum* compounds and synthesis of improved derivatives that confer anti-cancer activities *in vitro*. Front Pharmacol 2019;10:115. https://doi.org/10.3389/fphar.2019.00115
17. White TJ, Bruns T, Lee S, Taylor J. Amplification and direct sequencing of fungal ribosomal rna genes for phylogenetics. In: PCR Protocols. Elsevier; 1990. p. 315–22. http://doi.org/10.1016/B978-0-12-372180-8.50042-1
18. Sulaiman SQ, al Anbagi RA, Alshuwaili FRH, Abdalrahman AS. New records of three Basidiomycetous species from Iraq using phenotypic and phylogenetic analyses. Plant sci today. 2024;11(4):1047–54. https://doi.org/10.14719/pst.4416
19. Prasad R, Varshney VK, Harsh NSK, Kumar M. Antioxidant capacity and total phenolics content of the fruiting bodies and submerged cultured mycelia of sixteen higher basidiomycetes mushrooms

from India. Int J Med Mushrooms. 2015;17(10):933–41. https://doi.org/10.1615/IntJMedMushrooms.v17.i10.30

20. Subedi K, Basnet BB, Panday R, Neupane M, Tripathi GR. Optimization of growth conditions and biological activities of Nepalese *Ganoderma lucidum* strain Philippine. Adv Pharmacol Pharm Sci 2021;2021(12):1-7 https://doi.org/10.1155/2021/4888979
21. Yassin MA, Elgorban AM, El-Samawaty AERMA, Almunqedhi BMA. Biosynthesis of silver nanoparticles using *Penicillium verrucosum* and analysis of their antifungal activity. Saudi J Biol Sci 2021; 28 (4):2123–127. https://doi.org/10.1016/j.sjbs.2021.01.063
22. Wang D, Xue B, Wang L, Zhang Y, Liu L, Zhou Y. Fungus-mediated green synthesis of nano-silver using *Aspergillus sydowii* and its antifungal/antiproliferative activities. Scientific Reports. 2021; 11 (1). https://doi.org/10.1038/s41598-021-89854-5
23. Ahmad K, Asif HM, Afzal T, Khan MA, Younus M, Khurshid U, et al. Green synthesis and characterization of silver nanoparticles through the *Piper cubeba* ethanolic extract and their enzyme inhibitory activities. Front Chem. 2023;11:1065986. https://doi.org/10.3389/fchem.2023.1065986
24. Jaast S, Grewal A. Green synthesis of silver nanoparticles, characterization and evaluation of their photocatalytic dye degradation activity. Curr Res Green Sustain Chem. 2021;4:100195. https://doi.org/10.1016/j.crgsc.2021.100195
25. Mohammed Ali IM, Ahmed AB, Al-Ahmed HI. Green synthesis and characterization of silver nanoparticles for reducing the damage to sperm parameters in diabetic compared to metformin. Scientific Reports. 2023;13(1). https://doi.org/10.1038/s41598-023-29412-3
26. Chand K, Abro MI, Aftab U, Shah AH, Lakhan MN, Cao D, et al. Green synthesis characterization and antimicrobial activity against: *Staphylococcus aureus* of silver nanoparticles using extracts of neem, onion and tomato. RSC Advances. 2019;9 (30):17002–015. https://doi.org/10.1039/c9ra01407a
27. Aspoukeh PK, Barzinjy AA, Hamad SM. A novel approach to the green synthesis of zinc oxide nanorods using *Thymus kotschyanus* plant extract: effect of ammonium hydroxide and precursor concentration. Nano Ex. 2023; 4(4). https://doi.org/10.1088/2632-959X/acfe25
28. Al-Hayanni HSA, Alnuaimi MT, Al-Lami RAH, Zaboon SM. Antibacterial effect of silver nanoparticles prepared from *Sophora flavescens* root aqueous extracts against multidrug-resistance *Pseudomonas aeruginosa* and *Staphylococcus aureus*. Journal of Pure and Applied Microbiology. JPAM. 2022; 16(4):2880–890. https://doi.org/10.22207/JPAM.16.4.61
29. Keshari AK, Srivastava R, Singh P, Yadav VB, Nath G. Antioxidant and antibacterial activity of silver nanoparticles synthesized by *Cestrum nocturnum*. J-AIM. 2020;11(1):37–44. https://doi.org/10.1016/j.jaim.2017.11.003
30. Sharma A, Sagar A, Rana J, Rani R. Green synthesis of silver nanoparticles and its antibacterial activity using fungus *Talaromyces purpureogenus* isolated from Taxus baccata Linn. Micro nano syst. lett. 2022;10(1). https://doi.org/10.1186/s40486-022-00144-9
31. Giusti A, Ricci E, Tinacci L, Verdigi F, Narducci R, Gasperetti L, et al. Molecular authentication of mushroom products: First survey on the Italian market. Food Control. 2023; 150(4):109778. https://doi.org/10.1016/j.foodcont.2023.109778
32. Rajurkar A, Gogri D, Jamdade N, Pathak A. Green synthesis of silver nanoparticles: their characterization, antimicrobial, antioxidant activity and nanogel formulation. Nano Biomed. Eng. 2023; 15(1):42–50. http://doi.org/10.26599/NBE.2023.9290006
33. Sreenivasagan S, Subramaniann A, Rajeshkumar S. Uv-Vis spectroscopy of silver nanoparticles and toxicology evaluation of silver nanoparticle based oral rinse on embryonic development of Zebrafish. J Complement Med Res. 2021; 12(2):85-90. http://doi.org/10.5455/jcmr.2021.12.02.12
34. 34. Pacheco-Coello F. Synthesis and size estimation of silver nanoparticles, by reduction with aqueous extracts of calyces leaves and seeds of *Hibiscus sabdariffa linn*: Promotion of green synthesis. Rev Bol Quim. 2021;38(3):113-18. http://www.bolivianchemistryjournal.org/
35. Mustapha T, Ithnin NR, Othman H, Abu Hasan ZI, Misni N. Biofabrication of silver nanoparticles using *Citrus aurantifolia* fruit peel extract (CAFPE) and the role of plant extract in the synthesis. Plants. 2023; 12(8). https://doi.org/10.3390/plants12081648
36. El-Mehdawy AA, Koriem M, Amin RM, Shehata AZI, El-Naggar HA. Green synthesis of silver nanoparticles using chitosan extracted from *Penaeus indicus* and its potential activity as aquatic larvicidal agent of *Culex pipens*. Egypt J Aquat Biol Fish. 2022; 26 (1):425-42. https://doi.org/10.21608/EJABF.2022.219887
37. Nkosi NC, Basson AK, Ntombela ZG, Dlamini NG, Pullabhotla RVSR. Green synthesis, characterization and application of silver nanoparticles using bioflocculant: a review. Bioengineering. 2024; 11(5):492. https://doi.org/10.3390/bioengineering11050492
38. Alabi IY, Adenipekun CO, Ipeaiyeda RA, Adekanmbi AO, Adebayo-Tayo AB. Antibacterial activities of biosynthesized silver-nanoparticles from three species of mushroom. Afr J Biomed Res. 2024;27(1):161–68. https://doi.org/10.4314/ajbr.v27i1.X
39. Qamer S, Che-Hamzah F, Misni N, Joseph NMS, Al-Haj NA, Amin-Nordin S. Deploying a novel approach to prepare silver nanoparticle *Bellamya bengalensis* extract conjugate coating on orthopedic implant biomaterial discs to prevent potential biofilm formation. Antibiotics. 2023;12(9). https://doi.org/10.3390/antibiotics12091403
40. Nahar K, Hafezur Rahaman M, Arifuzzaman Khan GM, Khairul Islam Md, Al-Reza SM. Green synthesis of silver nanoparticles from *Citrus sinensis* peel extract and its antibacterial potential. AJGC. 2021; 5(1):135–50. https://doi.org/10.22034/ajgc.2021.113966
41. Sweedan EG, Abdul Majeed SM. Effects of silver nanoparticles synthesized from phenolic extract of *Agaricus bisporus* against pathogenic bacteria and yeasts. Nano Biomed Eng. 2023;15(1):86–95. https://doi.org/10.26599/NBE.2023.9290010
42. Robinson M, Filice CT, McRae DM, Leonenko Z. Atomic force microscopy and other scanning probe microscopy methods to study nanoscale domains in model lipid membranes. Adv Phys X. 2023;8(1):2197623. https://doi.org/10.1080/23746149.2023.2197623
43. Nasiri S, Rabiei M, Palevicius A, Janusas G, Vilkauskas A, Nutalapati V, et al. Modified Scherrer equation to calculate crystal size by XRD with high accuracy, examples Fe_2O_3, TiO_2 and V_2O_5. Nano Trends. 2023; 3,100015, p. 1-12. https://doi.org/10.1016/j.nwnano.2023.100015
44. Kuru M, Kuru TŞ, Karaca E, Bağcı S. Dielectric, magnetic and humidity properties of Mg–Zn–Cr ferrites. J Alloys Compd. 2020;836, 155318. https://doi.org/10.1016/j.jallcom.2020.155318
45. Abbas R, Luo J, Qi X, Naz A, Khan IA, Liu H, et al. Silver nanoparticles: synthesis, structure, properties and applications. Nanomaterials. 2024;14(17):1425. https://doi.org/10.3390/nano14171425
46. Irwan R, Teheni MT, Syafriah W. Synthesis and characterization of silver nanoparticles from the leaf stalk extract of *Moringa oleifera*. Indo J Chem Res. 2023;11(1):37–42. https://doi.org/10.30598//ijcr.2023.11-irw
47. Almatroudi A. Silver nanoparticles: Synthesis, characterisation and biomedical applications. Open Life Sci. 2020; 15(1):819–39. https://doi.org/10.1515/biol-2020-0094
48. Okumus E. Green synthesis of silver nanoparticles using *Hebeloma excedens* mushroom extract as a new source: Anti-lipid peroxidation, bioaccessibility and antidiabetic properties. J Food Meas Charact. 2024;18(6):5157–169. https://doi.org/10.1007/s11694-024-02635-2

49. Alzubaidi AK, Al-Kaabi WJ, Ali A al, Albukhaty S, Al-Karagoly H, Sulaiman GM, et al. Green synthesis and characterization of silver nanoparticles using flaxseed extract and evaluation of their antibacterial and antioxidant activities. Appl Sci. 2023;13(4). https://doi.org/10.3390/app13042182

50. Ohiduzzaman, Khan MNI, Khan KA, Bithi P. Biosynthesis of silver nanoparticles by banana pulp extract: Characterizations, antibacterial activity and bioelectricity generation. Heliyon. 2024; 10(3):e25520. https://doi.org/10.1016/j.heliyon.2024.e25520

51. Ipe DS, Kumar PTS, Love RM, Hamlet SM. Silver nanoparticles at biocompatible dosage synergistically increases bacterial susceptibility to antibiotics. Front Microbiol. 2020;11:1074. https://doi.org/10.3389/fmicb.2020.01074

52. González-Fernández S, Lozano-Iturbe V, García B, Andrés LJ, Menéndez MF, Rodríguez D, et al. Antibacterial effect of silver nanorings. BMC Microbiology. 2020;20(1):172. https://doi.org/10.1186/s12866-020-01854-z

53. Holubnycha V, Husak Y, Korniienko V, Bolshanina S, Tveresovska O, Myronov P, Holubnycha M, et al. Antimicrobial activity of two different types of silver nanoparticles against wide range of pathogenic bacteria. Nanomaterials. 2024; 14(2):137. https://doi.org/10.3390/nano14020137

54. More PR, Pandit S, Filippis A de, Franci G, Mijakovic I, Galdiero M. Silver nanoparticles: bactericidal and mechanistic approach against drug resistant pathogens. Microorganisms. 2023; 11 (2):369. https://doi.org/10.3390/microorganisms11020369

55. Pazos-Ortiz E, Roque-Ruiz JH, Hinojos-Márquez EA, López-Esparza J, Donohué-Cornejo A, Cuevas-González JC, et al. Dose-dependent antimicrobial activity of silver nanoparticles on polycaprolactone fibers against gram-positive and gram-negative bacteria. J Nanomater. 2017;2017(6):1-9. https://doi.org/10.1155/2017/4752314

56. Dakal TC, Kumar A, Majumdar RS, Yadav V. Mechanistic basis of antimicrobial actions of silver nanoparticles. Front Microbiol 2016; 7:1831. https://doi.org/10.3389/fmicb.2016.01831

57. Salari S, Bahabadi E, Samzadeh-Kermani A, Yosefzaei F. *In-vitro* evaluation of antioxidant and antibacterial potential of green synthesized silver nanoparticles using *Prosopis farcta* fruit extract. Iran J Pharm Res. 2019;18(1):430-45. https://doi.org/10.22037/ijpr.2019.2330

58. Ansar S, Tabassum H, Aladwan NSM, Naiman Ali M, Almaarik B, AlMahrouqi S, et al. Eco friendly silver nanoparticles synthesis by *Brassica oleracea* and its antibacterial, anticancer and antioxidant properties. Scientific Reports. 2020;10(1). https://doi.org/10.1038/s41598-020-74371-8